J Mater Sci: Mater Med (2008) 19:777–788
DOI 10.1007/s10856-006-0051-8

Latex of immunodiagnosis for detecting the Chagas disease. I. Synthesis of the base carboxylated latex

Verónica D. G. Gonzalez · Luis M. Gugliotta · Gregorio R. Meira

Received: 6 April 2006 / Accepted: 20 November 2006 / Published online: 16 August 2007

Abstract This article investigates the synthesis of two (monodisperse, carboxylated, and core-shell) latexes, through a batch and a semibatch emulsion copolymerizations of styrene (St) and methacrylic acid (MAA) onto polystyrene latex seeds. A mathematical model of the process was developed that predicts conversion, average particle size, and surface density of carboxyl groups. The model was adjusted to the batch reaction measurements, and then it was used in the design of the semibatch experiment. The semibatch reaction involved an initial homopolymerization of St followed by instantaneous addition of MAA-St-initiator. Compared with the batch reaction results, the semibatch policy more than doubled the surface density of carboxyl groups. The second part of this series describes the development of an immunodiagnosis latex–protein complex for detecting the Chagas disease, by coupling an antigen of *Trypanosoma cruzi* onto the produced carboxylated latexes.

Nomenclature

A or MAA	methacrylic acid monomer.
$A_1^{\cdot}$, $S_1^{\cdot}$	Primary A and S radicals.
$A_n^{\cdot}$, $S_n^{\cdot}$	A- and S-ended radicals of chain length n.
A_p	Total area of polymer particles [cm^2].
C_{NaOH}	NaOH concentration [mEq/g].
$\bar{D}$	Average particle diameter [nm].
f	Initiation efficiency.
F	Faraday constant [μC/mEq].
$F_{i,\ in}$	Inlet molar flow rate of species i [mol/s].
f_S	Molar fraction of St with respect to the total monomer.
h	Depth of the external particle shell where the reactive ($SO_4^{=}$ and COOH) groups are accessed by the conductimetric titration [nm].
I_2	Water-soluble initiator.
$[i]_j$	Concentration of comonomer i in phase j [mol/cm^3].
k_a	Rate constant of radical absorption into the polymer particles [cm^3/mol s].
k_d	Rate constant of initiator decomposition [s^{-1}].
k_{de}	Rate constant of radical desorption from the polymer particles [s^{-1}].
k_{fij}	Transfer rate constant between an i-ended propagating radical and a j-monomer [cm^3/mol s].
k_{pSS}, k_{pAA}	Homopropagation rate constants of S and A [cm^3/mol s].
k_{pAS}, K_{pSA}	Cross-propagation rate constants [cm^3/mol s].
k_{pcS}, k_{pcA}	Rate of generation of primary monomeric radicals.

V. D. G. Gonzalez · L. M. Gugliotta · G. R. Meira (✉)
INTEC (Universidad Nacional del Litoral and CONICET), Güemes 3450, 3000 Santa Fe, Argentina
e-mail: gmeira@ceride.gov.ar

V. D. G. Gonzalez
e-mail: veronikg@ceride.gov.ar

L. M. Gugliotta
e-mail: lgug@intec.unl.edu.ar

k_{tp}	Rate constant of global termination in the polymer phase [cm^3/mol s].
k_{tw}	Rate constant of global termination in the aqueous phase [cm^3/mol s].
K_i^m	Partition coefficient of comonomer i between the monomer and the aqueous phases.
K_i^p	Partition coefficient of comonomer i between the polymer and the aqueous phases.
m_s	Total latex mass [g].
M_i	Molecular weight of comonomer i [g/mol].
$m_{NaOH,\,SO_4^=}$, $m_{NaOH,\,COOH}$	Mass of NaOH required for neutralizing the $SO_4^=$ and COOH reactive groups, respectively [g].
$\bar{n}$	Average number of free-radicals per particle.
N_{Av}	Avogadro's constant.
N_i	Moles of species i (i = A, S, I).
N_p	Total number of polymer particles.
$N_{i,b}$	Total moles of bound (or polymerized) comonomer i.
$N_{i,b}^w$	Moles of bound (or polymerized) comonomer i in the aqueous phase.
P_n	Dead polymer of chain length n.
r_S, r_A	Reactivity ratios of St and MAA, respectively.
$R_c^{\cdot}$	Primary initiator radical.
$R_n^{\cdot}$	Free-radical of chain length n, representing either $S_n^{\cdot}$ or $A_n^{\cdot}$.
R_{pi}^j	Rate of polymerization of comonomer i in phase j [mol/cm^3 s].
$[R^{\cdot}]_w$	Total concentration of free-radicals in the aqueous phase [mol/cm^3].
S or St	Styrene monomer.
V^j	Total volume of phase j [cm^3].
V_{pol}	Total dry polymer volume [cm^3].
v_i	Molar volume of comonomer i [cm^3/mol].
V_i	Total volume of comonomer i [cm^3].
V_i^j	Total volume of comonomer i in phase j [cm^3].
V_W^w	Total volume of water in the aqueous phase [cm^3].
w_s	Solid content or weight fraction of polymer [%].
x	Global mass conversion.
x^j	Global mass conversion in phase j.
x_i	Global conversion of comonomer i.
x_i^j	Conversion of comonomer i in phase j.
$X_{i,\,h}$	Average molar fraction of comonomer i in the copolymer contained in an external shell of depth h.
X_i	Molar fraction of comonomer i in the total copolymer.
X_i^j	Molar fraction of comonomer i in the copolymer produced in phase j.
$X_{i,\,inst}$	Instantaneous molar fraction of comonomer i in the global copolymer.
$X_{i,\,inst}^j$	Instantaneous molar fraction of comonomer i in the copolymer being produced in phase j.

Greek Symbols

$\delta_{SO_4^=,h}$, $\delta_{COOH,h}$	Density of sulfate and carboxyl groups in an external shell of depth h [mEq/cm^2].
ϕ_i^m	Volume fraction of comonomer i in the monomer phase.
ϕ_i^p	Volume fraction of comonomer i in the polymer droplets phase.
ρ_s	Dry polymer density [g/cm^3].
σ	Surface charge density [μC/cm^2].

Introduction

Polymer latexes are base materials for producing immunoassay (or immunodiagnosis) latex–protein complexes [1–11]. The base latexes are typically polystyrene (PS) particles of a narrow particle size distribution (PSD), containing functionalized reactive groups such as aldehyde [12, 13], amino [14, 15], carboxyl [16–22], hydroxyl [23], chloromethyl [15, 24, 25], and acetal [13, 15, 26]. Immunodiagnosis latex–protein complexes are produced by binding specific proteins onto the base functionalized

latexes. The latex–protein complexes must be stable and with a homogenous distribution of proteins. To this effect, the base functionalized latexes must be uniform in their particle sizes, and with a uniform distribution of external functional groups [27]. Proteins are bound onto functionalized latex by physical adsorption and/or by chemical linkage. The chemical linkage is preferable, since it improves the latex stability and protein orientations, thus reducing the risk of protein denaturing [28]. Immunodiagnosis tests are easily visualized agglutination reactions.

Functionalized latexes are typically produced in emulsion copolymerizations [29–32, 33]. In the unseeded emulsion process, the main hydrophobic comonomer (e.g., styrene) is polymerized in the presence of small quantities of a hydrophilic functionalization comonomer. In the seeded (or multistage) process, the core-shell morphologies are obtained by polymerizing one or more comonomers in the presence of a uniform latex seed. In this case, no new polymer particles are generated, and their final diameters are produced by a simple growth of the original seed. Typically, the seeds are PS latexes produced in emulsifier-free emulsion homopolymerizations of styrene (St).

At present, many functionalized latexes of varying sizes and surface densities are commercially available [34]. Bastos-González et al. [16] produced a carboxylated latex through a surfactant-free emulsion polymerizations of St with an azo-initiator. The carboxyl groups were at the polymer chain ends, and were provided by the initiator remnants. Lee et al. [17] copolymerized methyl methacrylate and methacrylic acid (MAA) onto a poly (methyl methacrylate) seed, to produce core-shell latexes with controlled concentrations of external carboxyl groups. Dos Santos et al. [20] copolymerized St and *n*-butyl acrylate in the presence of acrylic and MAAs; and analyzed the effects of pH on the distribution of the carboxyl groups between the particles surface, the particles core, and the aqueous phase. Slawinski et al. [21, 22] copolymerized St and acrylic acid onto a PS seed, observing an increased density of carboxyl groups at pH = 2.5. With respect to an equivalent batch copolymerization, the final density of carboxyl groups were increased by 35%, through an impulsive addition (or shot) of acrylic acid in the last stage of the reaction [22]. Also, when the functionalization comonomer is added near to the end of the reaction, it was recommended to add it mixed with the main comonomer, rather than pure [33, 35, 36].

Mathematical models of emulsion copolymerizations are useful for evaluating alternative reaction strategies, and for interpreting the complex physical-chemistry of such processes [37, 38]. For producing constant composition copolymers, semibatch strategies have been developed with the help of representative mathematical models [39–49].

This work describes a batch and a semibatch emulsion copolymerizations of St and MAA onto a PS seed, for producing two core-shell latexes with external carboxyl groups. The process model was adjusted to the batch reaction measurements. The semibatch reaction aimed at increasing the final surface density of carboxyl groups with respect to the batch.

Experimental methods

Base PS seeds

The seeds were two almost-uniform PS latexes. They were obtained in emulsifier-free emulsion homopolymerizations of St [50]. The recipes and final latex characteristics are in Table 1. Both seeds contained $SO_4^{=}$ groups at the chain ends, that correspond to the remnants of the persulfate initiator. The average particle diameters were determined by dynamic light scattering (DLS); and the final mass fraction of solids (or solid content) w_s was determined by gravimetry. The PSDs were almost monodisperse. In latex S1, the combined measurements of transmission electron microscopy (TEM), DLS, and UV–Vis turbidimetry suggested a main population of particles of an average diameter 348 nm, contaminated with 1% in weight of larger particles [51].

Reaction system

A 1-L jacketed glass reactor was used, fitted with a stainless-steel stirrer and a thermostatic bath. The reactor connectors permitted the continuous bubbling of nitrogen, the semibatch addition of reagents, and taking samples along the reaction.

The reaction recipes are in Table 2. The St monomer (technical grade, Petrobras Energía S.A., Argentina) was vacuum distilled to eliminate inhibitors and other impurities. The MAA monomer (Merck, purity >99%), and the potassium persulfate initiator $K_2S_2O_8$ (Mallinckrodt, purity >99%), were used as received. The water was filtered and deionized. Latexes S1 and S2 were the seeds of the batch and semibatch copolymerizations, respectively.

Table 1 Base PS seeds: recipes and final latex characteristics [51]

	Seed S1	Seed S2
Recipe		
St (g)	49.76	41.61
$K_2S_2O_8$ (g)	0.6059	0.7190
Deionized H_2O (g)	750.30	750.09
Final latex characteristics		
$\bar{D}$ (nm)	349.7	347.1
w_s (%)	2.69	2.63

Table 2 Batch and semibatch reactions: reaction conditions, recipes, and final latex characteristics

	Batch reaction	Semibatch reaction
Temperature	70 °C	70 °C
Total reaction time	10 h	10 h
Recipe at t = 0 h		
PS seed	50 g of latex S1[a]	50 g of latex S2[a]
St	0.8160 g	0.8160 g
MAA	0.1380 g	–
$K_2S_2O_8$	0.2618 g	0.2618 g
H_2O deionized	449 g	449 g
		Injection at t = 4 h
		St: 0.1305 g
		MAA: 0.1380 g
		$K_2S_2O_8$: 0.2618 g
Final latex characteristics		
w_s [b]	0.066%	0.158%
x	77.2%	87.5%
$\bar{D}$	403.6 nm	417.7 nm
$\delta_{SO_4^=,\,h}$	0.043×10^{-8} mEq/cm^2	0.536×10^{-8} mEq/cm^2
$\delta_{COOH,\,h}$	1.682×10^{-8} mEq/cm^2	3.828×10^{-8} mEq/cm^2
σ	1.623 μC/cm^2	3.694 μC/cm^2
c.c.c. with KBr at pH = 6		
by visual method	200 mM	450 mM
by DLS	40 mM	200 mM

[a] Seed characteristics in Table 1

[b] Polymer mass fraction by gravimetry, after operation of serum replacement

After the reactions, the unreacted comonomers and initiator were eliminated in serum replacement operations. These operations involved a 1:4 dilution in the batch reaction sample, and a 1:1.6 dilution in the semibatch reaction sample. The final solid contents are in Table 2.

Measurements

For the samples taken along the reactions, the monomer conversion (x) was gravimetrically determined, and the average particle diameter ($\bar{D}$) was measured by DLS. For the DLS measurements, a light-scattering photometer by Brookhaven Instruments Inc. was employed, fitted with a vertically polarized He-Ne laser at 632.8 nm, and a digital correlator (Model BI-2000 AT).

For the two final and cleaned latexes, their density of external carboxyl groups was determined by conductimetry; and their critical coagulation concentration (*c.c.c.*) was determined by direct observation and by DLS.

For the conductivity measurements, the final samples were further diluted with ultra-pure water under magnetic agitation. Thus, 40 mL of the batch reaction sample were diluted into 200 mL; and 20 mL of the semibatch reaction sample were diluted into 200 mL. Then, 1 mL of a HCl solution (0.1 mEq/g) were added to each sample, to produce the complete protonation of the accessible acidic groups (corresponding to the sulfate groups from the persulfate initiator and to the carboxyl groups from the MAA units). The conductimeter was an YSI, model 34. The NaOH titration solution was incorporated in steps of 0.2 g, by means of a discontinuous dispenser; and the conductivity measurements were taken about 10 s after the injections. Figure 1 shows the titration curve of the batch reaction sample. The curve can be represented by three linear segments of different slopes, and m_1 and m_2 are the total added grams of NaOH at the changes of slope. The first segment corresponds to the neutralization of the (strong) HCl and sulfate protons; the second segment corresponds to the neutralization of the (weaker) carboxyl group protons; and the third segment corresponds to the NaOH in excess. The grams of NaOH for neutralizing the COOH groups are: $m_{NaOH,\,COOH} = m_2 - m_1$. The grams of NaOH for neutralizing the $SO_4^=$ groups are: $m_{NaOH,\,SO_4^=} = m_1 - m_{NaOH,\,ClH}$, where $m_{NaOH,\,ClH}$ are the grams of NaOH for neutralizing the (known) added amount of HCl.

The hard and viscous PS-based particles grow in a layer-by-layer fashion, and most of the internal sulfate and

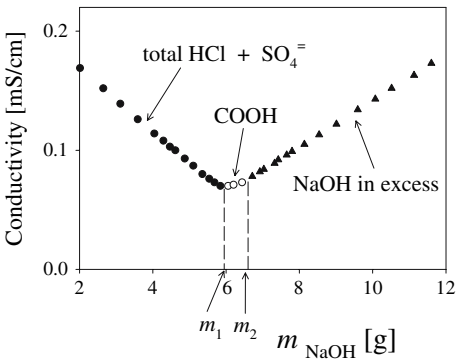

Fig. 1 Surface density of sulfate and carboxyl groups in the final batch reaction sample: Conductimetric titration. The masses m_1 and m_2 indicate the changes of slope

carboxyl groups remain inaccessible to the protonation-neutralization reactions. We assumed that the titrations neutralized all of the sulfate and carboxyl groups contained in an outer shell of (an unknown) depth h. The value of h was not measured, but it was considered an adjustable model parameter. Call $\delta_{SO_4^=,h}$ and $\delta_{COOH,h}$ (in mEq/cm^2), the measured surface densities of sulfate and carboxyl groups. The subscript h is introduced to highlight the fact that only the outer groups are neutralized. These densities were determined from:

$$\delta_{SO_4^=,h} = \frac{m_{NaOH,SO_4^=} C_{NaOH}}{A_p}; \qquad \delta_{COOH,h} = \frac{m_{NaOH,COOH} C_{NaOH}}{A_p} \tag{1}$$

with

$$A_p = \frac{6\, m_s\, w_s}{\rho_s\, \bar{D}} \tag{2}$$

where C_{NaOH} (= 2×10^{-2} mEq/g) is the titration solution concentration; A_p is the total surface of the unswollen particles, in cm^2; m_s is the total latex mass, in g; w_s are the g of solids per 100 g of latex; ρ_s is the dry polymer density, in g/cm^3; and $\bar{D}$ is the (unswollen) average particle diameter, determined by DLS (Table 2). Finally, the total density of surface charge (σ), in μC/cm^2, is given by:

$$\sigma = F\left(\delta_{SO_4^=,h} + \delta_{COOH,h}\right) \tag{3}$$

where F (= 96.5 μC/mEq) is the Faraday constant.

The *c.c.c.* was defined as the minimum concentration of KBr necessary for producing an incipient latex coagulation. This quantity is an indication of the latex stability, and it was determined as follows. Solid KBr from Cicarelli was used to prepare a 1 M standard solution; and then several solutions were obtained by dilution of such standard. A series of tubes were used for mixing 1 mL of latex (0.08 mg/mL) with 1 mL of the different KBr solutions. The tubes were maintained at 37 °C for 24 h and without agitation. The incipient coagulation was determined by direct observation and by DLS. The instrumental determinations proved more sensitive, thus yielding lower *c.c.c.* values (Table 2).

Batch copolymerization and mathematical model

The batch copolymerization recipe is in the second column of Table 2. First, the reactor was loaded with water, the S1 seed, and the comonomers. Then, the mixture was agitated for 2 h at 250 rpm and at room temperature, to saturate the seed particles with the comonomers. During this initial stirring period, nitrogen was bubbled to eliminate the dissolved oxygen. The total comonomers mass was small with respect to the seeds (Table 2). For that reason, it was assumed that at the start of the polymerization all the comonomers were swollen in the seed particles, and no independent monomer phase was present. To start the reactions, the temperature was raised to 70 °C, and the initiator solution was added.

Figure 2 presents the measurements (in open circles), and Table 2 presents the final latex characteristics. Note that the final (unswollen) average particle diameter was only 15% larger than the (also unswollen) average seed diameter.

The mathematical model is in the Appendix. It is similar to those presented in Salazar et al. [52] and Gugliotta et al. [53], and it is based on the kinetic mechanism of Table 3. The model assumptions are as follows: (a) the PSD is monodisperse; (b) the low molecular-weight species are distributed between the phases according to constant partition coefficients; (c) the comonomers are only consumed by the propagation reactions (long-chain hypothesis); (d) the total free-radical concentration varies slowly with time (pseudo steady-state hypothesis); (e) the polymer being produced in the aqueous phase, instantaneously precipitates onto the polymer particles; (f) the new dead polymer accumulates onto the particles surface in a layer-by-layer fashion, and the average copolymer composition in an outer shell of depth h is calculated by integration of the precipitated copolymer that accumulates in successive layers (see Eqs. A.32–34); and (g) the parameter h was adjusted from the measured density of carboxyl groups of the final batch reaction sample.

The following simplifications were adopted for the kinetic parameters. The homopropagations rate constants in the polymer phase were assumed identical to the homopropagations rate constants in the aqueous phase; and

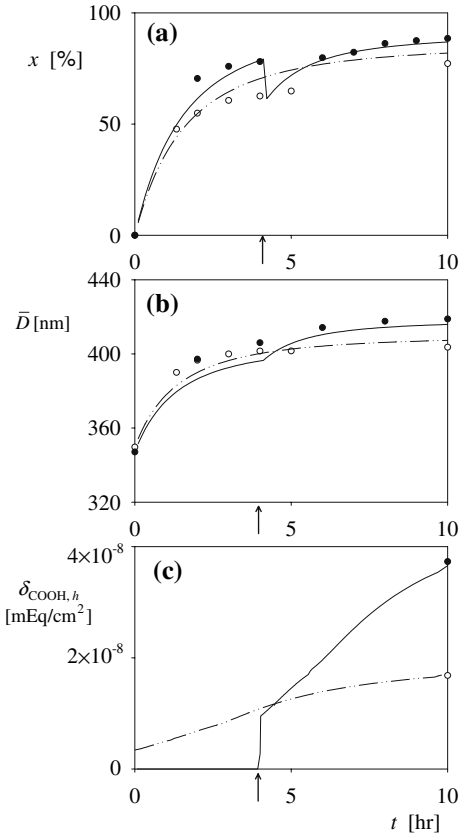

Fig. 2 Batch (○, –·–) and semibatch (•, —) reactions. Measurements and model predictions of: (**a**) the overall gravimetric conversion; (**b**) the unswollen average particle diameter; and (**c**) the surface density of carboxyl groups. The arrow indicates the semibatch impulsive injection of MAA, St, and initiator

Table 3 Emulsion copolymerization of St and MAA: kinetic scheme

Aqueous phase	Polymer phase
Initiation	
$I_2 \xrightarrow{k_d} 2\,R_c^{\cdot}$	
$R_c^{\cdot} + S \xrightarrow{k_{pcS}} S_1^{\cdot}$	
$R_c^{\cdot} + A \xrightarrow{k_{pcA}} A_1^{\cdot}$	
Propagation	*Propagation*
$S_n^{\cdot} + S \xrightarrow{k_{pSS}} S_{n+1}^{\cdot}$	$S_n^{\cdot} + S \xrightarrow{k_{pSS}} S_{n+1}^{\cdot}$
$A_n^{\cdot} + S \xrightarrow{k_{pAS}} S_{n+1}^{\cdot}$	$A_n^{\cdot} + S \xrightarrow{k_{pAS}} S_{n+1}^{\cdot}$
$S_n^{\cdot} + A \xrightarrow{k_{pSA}} A_{n+1}^{\cdot}$	$S_n^{\cdot} + A \xrightarrow{k_{pSA}} A_{n+1}^{\cdot}$
$A_n^{\cdot} + A \xrightarrow{k_{pAA}} A_{n+1}^{\cdot}$	$A_n^{\cdot} + A \xrightarrow{k_{pAA}} A_{n+1}^{\cdot}$
	Transfer to the monomer
	$S_n^{\cdot} + S \xrightarrow{k_{fSS}} P_n + S_1^{\cdot}$
	$S_n^{\cdot} + A \xrightarrow{k_{fSA}} P_n + A_1^{\cdot}$
	$A_n^{\cdot} + S \xrightarrow{k_{fAS}} P_n + S_1^{\cdot}$
	$A_n^{\cdot} + A \xrightarrow{k_{fAA}} P_n + A_1^{\cdot}$
Termination	*Termination*
$R_n^{\cdot} + R_m^{\cdot} \xrightarrow{k_{tw}} P_n + P_m$ or P_{n+m}	$R_n^{\cdot} + R_m^{\cdot} \xrightarrow{k_{tp}} P_n + P_m$ or P_{n+m}

similarly with the cross-propagation rate constants. For the termination reactions, pseudo-rate constants were adopted. In the polymer phase, the pseudo-rate termination was low and constant, due to the large and constant gel effect caused by the relatively small mass of initial comonomers with respect to the seed. In the aqueous phase, most of the free radicals are MAA-terminated, and for this reason the pseudo-termination was adopted constant and equal to the MAA termination. Finally, both the MAA- and St-terminated oligomeric radicals are absorbed and desorbed from the polymer particles at rates that coincide with the rates of the St-terminated radicals.

The mathematical model predicted the time evolution of the comonomer concentrations in all the phases (aqueous, monomer-droplets, and polymer), the phase volumes, the copolymer composition, the average particle diameter, and the average density of external carboxyl groups. The adopted parameters are in Table 4. Most of the parameters were directly taken from the literature, but k_{tp} and h were adjusted as follows. The global termination in the polymer phase (k_{tp}) was adjusted to fit the measurements of the global conversion and average particle diameter. The depth of the external shell layer up to where the sulfate and carboxyl groups were detected was adjusted to fit the measured final surface density of carboxyl groups. The resulting value of $h = 0.25$ nm (Table 4), suggests that most of the internal carboxyl groups remained inaccessible to the titration test.

At 70 °C, the partitions of St and MAA between the polymer and aqueous phases are 1200:1 and 3.6:1, respectively. In addition, the water phase volume is considerably larger than the polymer phase volume (Table 4). For these reasons, most of the unreacted MAA remains in the water phase but it reacts in the polymer phase, as is it explained below.

A reactivity ratio quantifies the tendency of a comonomer radical to homopolymerize vs. to crosspolymerize [Eqs. (A.21) and (A.22)]. In our particular reaction, both reactivity ratios are smaller than 1, and r_A is about four times larger than r_S (Table 4). Prior to analyzing our batch emulsion process, consider an equivalent batch copolymerization carried out in homogeneous conditions (e.g., in solution). Figure 3 represents the Mayo equation [59]. The instantaneous molar fraction of bound MAA in the copolymer $X_{A,\,inst}$ is represented vs. the instantaneous molar fraction of MAA in the comonomers mixture f_A. Point A with $f_A = 0.739$ represents the azeotropic composition, where a uniform copolymer composition is obtained. Point G_1 at $f_A = 0.178$ represents the global initial conditions of our equivalent homogeneous copolymerization. In this case, the instantaneous molar fraction of bound MAA in the copolymer $X_{A,\,inst}$ would decrease monotonically from 0.405 (at 0% conversion) to 0 (at 100% conversion).

Table 4 Model parameters

Parameter	Value	Reference
k_{pSS}, k_{pAA}, k_{pSA}, k_{pAS} (cm^3/mol s)	4.8×10^5; 6.0×10^5; 3.2×10^6; 8.57×10^5	[54]
r_S, r_A (dimensionless)	0.15; 0.70	[54]
k_{tp} (cm^3/mol s)	2.5×10^{11}	adjusted in this work
k_{tw} (cm^3/mol s)	2.7×10^{10} [a]	[54]
k_d (s^{-1})	1.147×10^{-4}	[55]
f (dimensionless)	0.6	[55]
k_a (cm^3/mol s)	3.20×10^{14}	[56]
k_{de} (s^{-1})	1.74×10^{-7}	[56]
K_S^m, K_S^p (dimensionless)	1800; 1200	[57, 58]
K_A^m, K_A^p (dimensionless)	6; 3.6	[55]
h (nm)	0.25	adjusted in this work[b]

[a] Adopted equal to the termination rate constant of the MAA homopolymerization

[b] With the final density of carboxyl groups of the batch copolymerization

Accordingly, the cumulative mass fraction of MAA in the copolymer is also expected to decrease monotonically.

For our emulsion batch process, Fig. 4a represents the evolution of the instantaneous molar fractions of MAA in the aqueous and polymer phases ($X^w_{A,\,inst}$ and $X^p_{A,\,inst}$, respectively); and Fig. 4b represents accumulated molar fraction of MAA in the global copolymer X_A. All of these functions are seen to increase monotonically. This behavior differs from that of the equivalent homogeneous copolymerization, but it is rather convenient for our purpose of maximizing the final surface density of carboxyl groups. To explain the emulsion behavior, note first that according to Fig. 4c, more than 99% of the total polymer is produced in the polymer particles. In addition, the MAA concentration in the polymer particles is essentially constant, because a mass transfer of MAA from the aqueous into the polymer phase replaces most of the reacted MMA. The St monomer shows a similar behavior, but in a reduced scale (while 87% of the total reacted MAA is transferred from the aqueous phase into the polymer phase; only 17% of the total reacted St is transferred). This is indirectly shown in Fig. 4d–f: while the moles of MAA in the water phase is about 2 orders of magnitude larger than in the polymer phase, for St the same ratio is about 1/5. In summary, the global copolymer increases its MAA content along the emulsion process because in the polymer phase (where most of the polymerization takes place) the MAA concentration decreases more slowly than the St concentration.

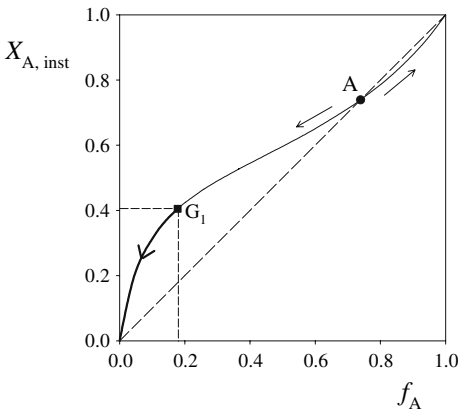

Fig. 3 Homogeneous batch copolymerization of St and MAA at 70 °C, according to the Mayo equation [54]. The instantaneous molar composition of MAA in the copolymer ($X_{A,\,inst}$) is represented vs. the instantaneous molar fraction of MAA in the reaction mixture (f_A). G_1 represents the initial reaction condition, and A is the azeotropic composition

Semibatch reaction and discussion of results

The semibatch experiment was designed to increase the final density of carboxyl groups with respect to the batch reaction. The recipe is in the third column of Table 2. First, the reactor was charged with water, the S2 seed, and most of the St monomer. Then, the mixture was stirred under nitrogen at room temperature for 2 h, to swell the particles with St. Finally, the temperature was raised to 70 °C, and the first load of initiator solution was loaded to start the St homopolymerization. After 4 h of reaction (when according to the model the St conversion was around 75%), two shots were injected: a mixture of equal masses of both comonomers and the second load of initiator solution (Table 2). The MAA was not added pure, to avoid producing poly(MAA) homopolymer, that would tend to remain in solution rather than precipitating onto the

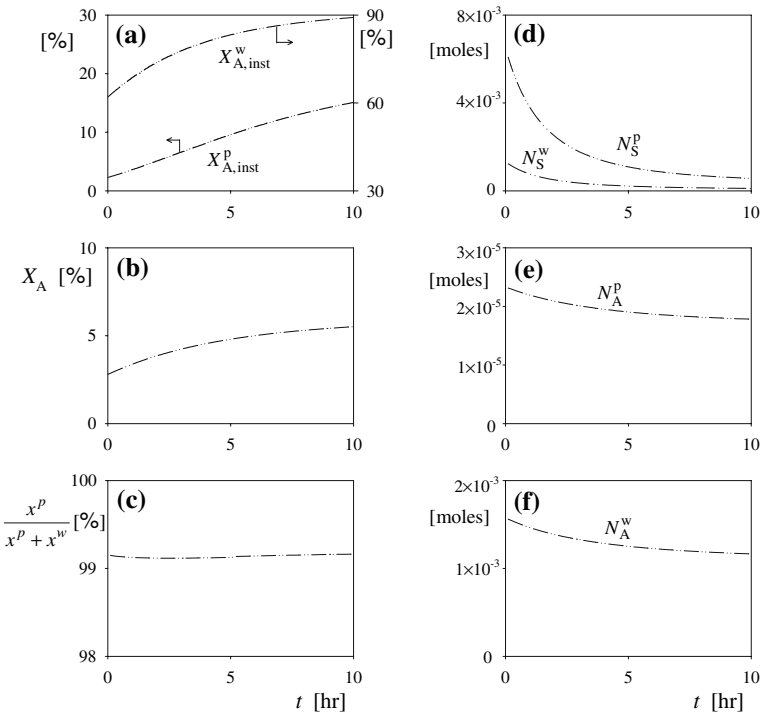

Fig. 4 Batch copolymerization: evolution of the global chemical composition (simulation results). (**a**) Instantaneous molar composition of MAA of the copolymer produced in the polymer phase and in the aqueous phase; (**b**) cumulative molar fraction of MAA in the total copolymer; (**c**) mass fraction of polymer produced in the polymer phase; (**d**) unreacted moles of St in the polymer and aqueous phases; and (**e**, **f**) unreacted moles of MAA in the polymer and aqueous phases

particles surface [33]. The second load of the persulfate initiator aimed at: (1) increasing the final conversion with respect to the batch reaction (for equal total reaction times of 10 h); and (2) increasing the final surface density of terminal $SO_4^{=}$ (the initiator remnants). In addition, the second load of initiator will reduce the final molecular weights.

The full circles in Fig. 2 represent the semibatch measurements, and the final latex characteristics are in the third column of Table 2. The model predictions of Figs. 2 and 5 were available prior to carrying out the semibatch experiment. The main result was that (in the clean and final latex, the surface density of carboxyl groups ($\delta_{COOH,\,h} = 3.8 \times 10^8$ mEq/cm^2), almost doubles the batch reaction value (Table 2 and Fig. 2c). Also, the model prediction for $\delta_{COOH,\,h}$ is very close to the corresponding measurement (Fig. 2c).

The homopolymerization of St is faster than the copolymerization of St and MAA [60]; and this explains that after 4 h of reaction, the conversion of the semibatch reaction was higher than that of the batch reaction (Fig. 2a). The second load of initiator not only increased the final semibatch reaction conversion (and therefore the average particle diameter) with respect to the batch (Fig. 2a, b); but also the final density of terminal $SO_4^{=}$ groups $\delta_{SO_4^{=},\,h}$ (Table 2). Finally, note the more than doubled values of the overall density of hydrophilic groups (σ), and of the *c.c.c.* (Table 2).

Figure 5 shows some final model predictions. Figure 5a presents the global St and MAA conversions. In the aqueous phase, the conversions are negligible with respect to the conversions in the polymer phase. Also, the final MAA conversions in the water phase (x^{w}_{A}) are one order of magnitude higher than the final St conversions in the water phase (x^{w}_{S}) (Fig. 5b, c). Along the reaction, there is a continuous mass transfer of comonomers and polymer from the aqueous phase into the polymer phase. This explains the continuous increase of the (swollen) polymer phase volumes (V^{p}) from the initial (swollen) seed volumes (Fig. 5d). In the semibatch reaction, the comonomers injection at $t = 4$ h produces a large increase in the polymer phase volume, because (according to the model), they are instantaneously absorbed into the polymer particles. In the batch reaction, the free radicals concentration in the aqueous phase ($[R^{\cdot}]_w$) falls monotonically; while in the semibatch reaction it increases at $t = 4$ h, due to the second initiator load (Fig. 5e). The average number of radicals per particle ($\bar{n}$) was around 5 (Fig. 5f), and this value is consistent with the relatively large particle diameters. The semibatch reaction produced the highest final molar composition of bound MAA in an outer shell of depth h ($X_{A,\,h}$) (Fig. 5g). However, note that in the batch reaction, the final global average composition of MAA (X_A) is higher than the previous value (Fig. 5h).

Conclusions

With respect to the equivalent batch copolymerization, the impulsive injection of MAA, St, and initiator near

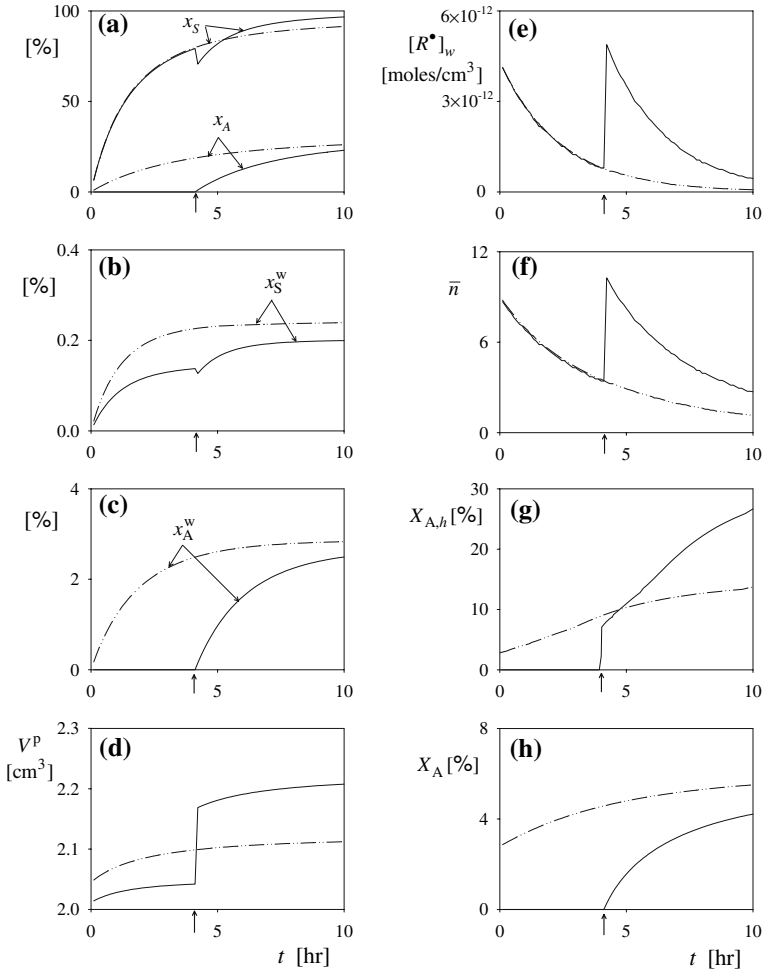

Fig. 5 Batch (–···–) and semibatch (——) reactions: more model predictions. (**a**) Global comonomer conversions; (**b, c**) comonomer conversions in the aqueous phase; (**d**) polymer phase volume; (**e**) concentration of free radicals in the aqueous phase; (**f**) average number of radicals per particle; (**g**) molar fraction of MAA in the copolymer contained in an outer layer of thickness h = 0.25 nm; and (**h**) molar fraction of MAA in the total copolymer. The arrow indicates the semibatch impulsive injection of initiator, MAA, and St

to the end of the semibatch reaction more than doubled the final density of carboxyl groups. This result improves that of Slawinski et al. [22], where a shot of AA near to the end of the reaction increased the density of carboxyl groups by 35% with respect to the batch.

In the batch reaction, the mathematical model helped understanding the increase of the MAA composition in the copolymer. (In an equivalent homogeneous copolymerization, the copolymer composition falls rather than increases.) In the semibatch reaction, the mathematical model was used to determining the optimal time for the St-MAA-initiator injection.

The second part of this work describes the sensitization of the produced latexes with an antigenic protein of *Trypanosoma cruzi*. The final aim was to develop an immunodiagnosis latex–protein complex for detecting the Chagas disease.

Acknowledgments We are grateful for the financial support received from CONICET, SeCyT, and Universidad Nacional del Litoral (Argentina).

Appendix: Mathematical model of a seeded emulsion copolymerization of St and MAA

Differential equations

From the kinetic scheme of Table 3, the following balances can be written for the moles of: comonomer i (N_i), of initiator (N_I), of total bound (or polymerized) comonomer i ($N_{i,b}$) with i = S, A, and of bound comonomer i in the phase j ($N_{i,b}^j$) with j = p, w:

$$\frac{dN_i}{dt} = F_{i,\,in} - R_{pi}^p V^p - R_{pi}^w V^w; \quad (i = S, A) \tag{A.1}$$

$$\frac{dN_I}{dt} = F_{I,\,in} - k_d N_I \tag{A.2}$$

$$\frac{dN_{i,b}}{dt} = R_{pi}^p V^p + R_{pi}^w V^w \tag{A.3}$$

$$\frac{dN_{i,b}^j}{dt} = R_{pi}^j V^j \tag{A.4}$$

where $F_{i,\mathrm{in}}$ and $F_{\mathrm{I,in}}$ are respectively the inlet molar flow rates of the comonomers (i = S, A), and of the initiator; $R^j_{\mathrm{p}i}$ is the polymerization rate of comonomer i in phase j (j = p, w); and V^j is the volume of phase j.

Algebraic equations

Assuming additivity of volumes, one can write:

$$V_i = V_i^{\mathrm{m}} + V_i^{\mathrm{w}} + V_i^{\mathrm{p}}; \quad (i = \mathrm{S},\ \mathrm{A}) \tag{A.5}$$

$$V^{\mathrm{w}} = V_{\mathrm{W}}^{\mathrm{w}} + V_{\mathrm{S}}^{\mathrm{w}} + V_{\mathrm{A}}^{\mathrm{w}} \tag{A.6}$$

$$V^{\mathrm{p}} = V_{\mathrm{S}}^{\mathrm{p}} + V_{\mathrm{A}}^{\mathrm{p}} + V_{\mathrm{pol}} \tag{A.7}$$

$$V^{\mathrm{m}} = V_{\mathrm{S}}^{\mathrm{m}} + V_{\mathrm{A}}^{\mathrm{m}} \tag{A.8}$$

where V_i is the total volume of comonomer i; V_i^{m}, V_i^{w}, and V_i^{p} are the total volumes of comonomer i in the monomer droplets phase, the aqueous phase, and the polymer particles phase, respectively; $V_{\mathrm{W}}^{\mathrm{w}}$ is the total water volume in the water phase; and V_{pol} is the (unswollen) total polymer volume.

The comonomers distribute themselves between the polymer, monomer, and aqueous phases, according the following constant partition coefficients:

$$\mathrm{K}_i^{\mathrm{p}} = \frac{\phi_i^{\mathrm{p}}}{\phi_i^{\mathrm{w}}}; \quad (i = \mathrm{S},\ \mathrm{A}) \tag{A.9a}$$

$$\mathrm{K}_i^{\mathrm{m}} = \frac{\phi_i^{\mathrm{m}}}{\phi_i^{\mathrm{w}}}; \quad (i = \mathrm{S},\ \mathrm{A}) \tag{A.9b}$$

with

$$\phi_i^j = \frac{V_i^j}{V^j}; \quad (i = \mathrm{S},\ \mathrm{A}) \text{ and } (j = \mathrm{p},\ \mathrm{m},\ \mathrm{w}) \tag{A.10}$$

where $\mathrm{K}_i^{\mathrm{p}}$ and $\mathrm{K}_i^{\mathrm{m}}$ are respectively the partition coefficients of comonomer i between the polymer phase and the aqueous phase, and between the monomer phase and the aqueous phase; and ϕ_i^j is the volume fraction of comonomer i in phase j.

From Eqs (A.5), (A.9), and (A.10), the following can be written:

$$V_i^{\mathrm{p}} = \frac{V_i}{1 + \frac{\mathrm{K}_i^{\mathrm{m}}}{\mathrm{K}_i^{\mathrm{p}}}\frac{V^{\mathrm{m}}}{V^{\mathrm{p}}} + \frac{1}{\mathrm{K}_i^{\mathrm{p}}}\frac{V^{\mathrm{w}}}{V^{\mathrm{p}}}}} \tag{A.11}$$

$$V_i^{\mathrm{w}} = \frac{1}{\mathrm{K}_i^{\mathrm{p}}}\frac{V^{\mathrm{w}}}{V^{\mathrm{p}}}V_i^{\mathrm{p}} \tag{A.12}$$

$$V_i^{\mathrm{m}} = \frac{\mathrm{K}_i^{\mathrm{m}}}{\mathrm{K}_i^{\mathrm{p}}}\frac{V^{\mathrm{m}}}{V^{\mathrm{p}}}V_i^{\mathrm{p}} \tag{A.13}$$

The molar concentration of comonomer i in phase j is:

$$[i]_j = \frac{V_i^j}{V^j}\frac{1}{\mathrm{v}_i}; \quad (i = \mathrm{S},\ \mathrm{A}) \tag{A.14}$$

where v_i is the molar volume of comonomer i.

In the aqueous phase, the mass balance for the total concentration of free radicals $[R^{\cdot}]_{\mathrm{w}}$, yields [61]:

$$2\,\mathrm{f}\,\mathrm{k_d}\,\frac{N_{\mathrm{I}}}{V^{\mathrm{w}}} + \mathrm{k_{de}}\frac{\bar{n}\mathrm{N_p}}{\mathrm{N_{Av}}V^{\mathrm{w}}} = \mathrm{k_a}[R^{\cdot}]_{\mathrm{w}}\frac{\mathrm{N_p}}{\mathrm{N_{Av}}V^{\mathrm{w}}} + 2\,\mathrm{k_{tw}}\,[R^{\cdot}]_{\mathrm{w}}^2 \tag{A.15}$$

where f is the initiation efficiency; $\bar{n}$ is the average number of free radicals per particle; $\mathrm{N_p}$ is the total number of polymer particles; $\mathrm{N_{Av}}$ is the Avogadro's constant; $\mathrm{k_{de}}$ is the rate constant of radical desorption from the polymer particles; and $\mathrm{k_a}$ is the rate constant of radical absorption into the polymer particles. In turn, $\bar{n}$ is given by [62]:

$$\bar{n} = 0.5\frac{2\alpha}{m + \frac{2\alpha}{m+1+\frac{2\alpha}{m+2+\cdots}}} \tag{A.16}$$

with

$$\alpha = \alpha' + m\bar{n} - \alpha^2 Y \tag{A.17}$$

$$\alpha' = \frac{2\,\mathrm{f}\,\mathrm{k_d}\,N_{\mathrm{I}}V^{\mathrm{p}}}{\mathrm{k_{tp}}\,\mathrm{N_p^2}}\mathrm{N_{Av}^2} \tag{A.18}$$

$$m = \frac{\mathrm{k_{de}}V^{\mathrm{p}}}{\mathrm{k_{tp}}\,\mathrm{N_p}}\mathrm{N_{Av}} \tag{A.19}$$

$$Y = \frac{2\,\mathrm{k_{tw}}\,\mathrm{k_{tp}}V^{\mathrm{w}}}{\mathrm{k_a^2}V^{\mathrm{p}}} \tag{A.20}$$

The reactivity ratios are defined by:

$$\mathrm{r_S} = \frac{\mathrm{k_{pSS}}}{\mathrm{k_{pSA}}} \tag{A.21}$$

$$\mathrm{r_A} = \frac{\mathrm{k_{pAA}}}{\mathrm{k_{pAS}}} \tag{A.22}$$

Then, the rates of comonomer consumption in each phase are obtained from:

$$R_{\mathrm{p}i}^{\mathrm{p}} = \frac{\bar{n}\mathrm{N_p}}{V^{\mathrm{p}}\mathrm{N_{Av}}}\left\{\frac{\mathrm{k_{pSS}}\,\mathrm{k_{pAA}}\left(\mathrm{r}_i[i]_{\mathrm{p}}^2 + [\mathrm{S}]_{\mathrm{p}}[\mathrm{A}]_{\mathrm{p}}\right)}{\mathrm{k_{pAA}}\,\mathrm{r_S}[\mathrm{S}]_{\mathrm{p}} + \mathrm{k_{pSS}}\,\mathrm{r_A}[\mathrm{A}]_{\mathrm{p}}}\right\} \quad (i = \mathrm{S},\ \mathrm{A}) \tag{A.23}$$

$$R_{pi}^{w} = [R^{\cdot}]_w \left\{ \frac{k_{pSS}\, k_{pAA} \left(r_i [i]_w^2 + [S]_w [A]_w \right)}{k_{pAA}\, r_S [S]_w + k_{pSS}\, r_A [A]_w} \right\} \quad (i = S, A) \tag{A.24}$$

After solving Eqs. (A.1–A.24), the following expressions calculate the global gravimetric conversion (x), the global conversion of comonomer i (x_i), the instantaneous molar composition of MAA units in the global copolymer ($X_{A,\,inst}$), the instantaneous molar composition of MAA units in the copolymer produced in the phase j ($X^j_{A,\,inst}$), the molar fraction of comonomer i in the total copolymer (X_i), the molar fraction of comonomer i in the copolymer contained in an outer shell of depth h ($X_{i,\,h}$), and the unswollen average particle diameter ($\bar{D}$):

$$x = \frac{M_S N_{S,b} + M_A N_{A,b}}{M_S (N_{S,b} + N_S) + M_A (N_{A,b} + N_A)} \tag{A.25}$$

$$x_i = \frac{N_{i,b}}{N_{i,b} + N_i} \quad (i = S, A) \tag{A.26}$$

$$X_{i,\,inst} = \frac{R_{pi}^{p} V^{p} + R_{pi}^{w} V^{w}}{R_{pS}^{p} V^{p} + R_{pS}^{w} V^{w} + R_{pA}^{p} V^{p} + R_{pA}^{w} V^{w}} \quad (i = S, A) \tag{A.27}$$

$$X^j_{i,\,inst} = \frac{R^j_{pi} V^j}{R^j_{pS} V^j + R^j_{pA} V^j} \quad (i = S, A) \text{ and } (j = p, w) \tag{A.28}$$

$$X_i = \frac{N_{i,b}}{N_{S,b} + N_{A,b}} \tag{A.29}$$

$$X_{i,\,h} = \frac{N_{i,b}\big|_h}{N_{S,b}\big|_h + N_{A,b}\big|_h} \tag{A.30}$$

$$\bar{D} = \left(\frac{6\, V_{pol}}{\pi N_p} \right)^{1/3} \tag{A.31}$$

where M_i is the molecular weight of comonomer i. The moles of bound comonomers contained in the outer shell of depth h are calculated from the difference between the total bound comonomers contained up to the external diameter $\bar{D}(t)$, and the total bound comonomers contained up to the internal diameter $(\bar{D} - h)(t)$, as follows:

$$N_{i,b}\big|_h = N_{i,b}\big|_{\bar{D}} - N_{i,b}\big|_{\bar{D}-h} \tag{A.32}$$

The total particle area (A_p) and the external density of carboxyl groups ($\delta_{COOH,\,h}$) are given by:

$$A_p = \pi \bar{D}^2 N_p \tag{A.33}$$

$$\delta_{COOH,\,h} = \frac{N_{A,b}\big|_h}{A_p} \times 10^3 = \frac{N_{A,b}\big|_{\bar{D}} - N_{A,b}\big|_{\bar{D}-h}}{A_p} \times 10^3 \tag{A.34}$$

Finally, the total gravimetric conversion in the phase j (x^j), the conversion of comonomer i in phase j (x^j_i), and the molar fraction of comonomer i in the copolymer produced in phase j (X^j_i), are given by:

$$x^j = \frac{M_S N^j_{S,b} + M_A N^j_{A,b}}{M_S (N_{S,b} + N_S) + M_A (N_{A,b} + N_A)} \quad (j = p, w) \tag{A.35}$$

$$x^j_i = \frac{N^j_{i,b}}{(N_{i,b} + N_i)} \quad (j = p, w) \tag{A.36}$$

$$X^j_i = \frac{N^j_{i,b}}{N^j_{S,b} + N^j_{A,b}} \quad (j = p, w) \tag{A.37}$$

References

1. C. PICHOT, T. DELAIR and A. ELAÏSSARI, in *Polymeric Dispersions: Principles and Applications*, edited by J. M. Asua, NATO ASI Series, Series E, Vol. 335(Dordrecht: Kluwer Academic Pub., 1997), p. 515
2. R. J. COHEN and G. B. BENEDEK, *Immunochemistry* **12** (1975) 349
3. G. QUAST, A. M. ROCH, A. NIVELEAU, J. GRANGE, T. KEOLOUANGKHOT and J. HUPPERT, *J. Immunol. Methods* **22** (1978) 165
4. W. J. LITCHFIELD, A. R. CRAIG, W. A. FREY, C. C. LEFLAR, C. E. LOONEY and M. A. LUDDY, *Clin. Chem.* **30** (1984) 1489
5. W. H. KAPMEYER, H. E. PAULY and P. TUENGLER, *J. Clin. Lab. Anal.* **2** (1988) 76
6. W. H. KAPMEYER, *Pure Appl. Chem.* **63** (1991) 1135
7. P. MONTAGNE, P. LAROCHE, M. L. CUILLIERE, P. VARCIN, B. PAU and J. DUHEILLE, *J. Clin. Lab. Anal.* **6** (1992) 24
8. T. BASINSKA and S. SLOMKOWSKI, in *Uses of Immobilized Biological Compounds*, edited by G. G. Guilbaut and M. Mascini (Netherlands, 1993)
9. J. M. PEULA, R. HIDALGO-ÁLVAREZ, R. SANTOS, J. FORCADA and F. J. DE LAS NIEVES, *J. Mater. Sci.: Mater. Med.* **6** (1995) 779
10. L. J. ORTEGA-VINUESA, J. A. MOLINA-BOLÍVAR and R. HIDALGO-ÁLVAREZ, *J. Immunol. Methods* **190** (1996) 29
11. J. SAROBE, I. MIRABALLES, J. A. MOLINA, J. FORCADA and R. HIDALGO-ÁLVAREZ, *Polym. Adv. Technol.* **7** (1996) 749
12. D. BASTOS-GONZÁLEZ, R. SANTOS-PÉREZ, J. FORCADA, R. HIDALGO-ÁLVAREZ and F. J. DE LAS NIEVES, *Colloid Surf. A* **92** (1994) 137
13. S. GIBANEL, V. HEROGUES, Y. GNANOU, E. ARAMENDIA, A. BUSCI and J. FORCADA, *Polym. Adv. Technol.* **12**(8) (2001) 494

14. TH. DELAIR, V. MARGUET, C. PICHOT and B. MANDRAND, *Colloid Polym. Sci*. **272** (1994) 962
15. M. P. SANZ IZQUIERDO, A. MARTÍN-MOLINA, J. RAMOS, A. RUS, L. BORQUE, J. FORCADA and F. GALISTEO-GONZÁLEZ, *J. Immunol. Methods* **287** (2004) 159
16. D. BASTOS-GONZÁLEZ, J. L. ORTEGA-VINUESA, F. J. DE LAS NIEVES and R. J. HIDALGO-ÁLVAREZ, *J. Colloid Interf. Sci*. **176** (1995) 232
17. C. F. LEE, T. H. YOUNG, Y. H. HUANG and W. Y. CHIU, *Polymer* **41** (2000) 8565
18. A. YU. MENSHIKOVA, T. G. EVSEEVA, YU. O. SKURKIS, T. B. TENNIKOVA and S. S. IVANCHEV, *Polymer* **46** (2005) 1417
19. K. KANG, C. KAN, Y. DU and D. LIU, *Eur. Polym. J*. **41** (2005) 439
20. A. M. DOS SANTOS, T. F. MCKENNA and J. GUILLOT, *J. Appl. Polym. Sci*. **65** (1997) 2343
21. M. SLAWINSKI, M. A. SCHELLEKENS, J. MEULDIJK, A. M. VAN HERK and A. L. GERMAN, *J. Appl. Polym. Sci*. **76** (2000) 1186
22. M. SLAWINSKI, J. MEULDIJK, A. M. VAN HERK and A. L. GERMAN, *J. Appl. Polym. Sci*. **78** (2000) 875
23. M. OKUBO, S. KAMEI, Y. TOSAKI, K. FUKUNAGA and T. MATSUMOTO, *Colloid Polym. Sci*. **265** (1987) 957
24. I. MIRABALLES-MARTÍNEZ, A. MARTÍN-RODRÍGUEZ and R. HIDALGO-ÁLVAREZ, *J. Biomater. Sci. – Polym. Ed*. **8**(10) (1997) 765
25. J. SAROBE, J. A. MOLINA-BOLÍVAR, J. FORCADA, F. GALISTEO and R. HIDALGO-ÁLVAREZ, *Macromolecules* **31**(13) (1998) 4282
26. R. M. SANTOS and J. FORCADA, *Prog. Colloid Polym. Sci*. **100** (1996) 87
27. L. TSAUR and R. M. FITCH, *J. Colloid Interf. Sci*. **115** (1987) 450
28. SERADYN Inc., *Procedures, Particle Technology, Microparticle Immunoassay Techniques* (Particle Technique División, 1988)
29. J. W. VANDERHOFF and H. J. VAN DEN HUL, *J. Macromol. Sci. Chem*. **A7**(3) (1973) 677
30. Z. SONG and G.W. POEHLEIN, *J. Colloid Interf. Sci*. **128**(2) (1989) 501
31. S. A. CHEN, S. T. LEE and S. J. LEE, *Makromol. Chem., Macromol. Symp*. **35/36** (1990) 349
32. W. D. HERGETH, K. SCHMUTZLER and W. SIEGFRIED, *Makromol. Chem., Macromol. Symp*. **31** (1990) 123
33. C. WANG, W. YANG and S. FU, in *Colloidal Polymers. Synthesis and Characterization*, edited by A. Elaissari, Surfactant Science Series, Vol. 115 (New York: Marcel Dekker, 2003), p. 93
34. www.bangslabs.com, www.seradyn.com
35. C. YAN, "Study of Ternary Emulsifier-free Emulsion Copolymerization and its Latex Particles as Support of Protein." PhD Dissertation (Hangzhou, China: Zhejiang University, 1998)
36. B. EMELIE, C. PICHOT and J. GUILLOT, *Makromol. Chem., Macromol. Chem. Phys*. **189** (1998) 1879
37. E. SALDIVAR, P. DAFNIOTIS and W. H. RAY, *J. Macromol. Sci., R. M. C*. **38** (1998) 207
38. J. GAO and A. PENDILIS, *Prog. Polym. Sci*. **27** (2002) 403
39. J. SNUPAREK and F. KRSKA, *J. Appl. Polym. Sci*. **21** (1977) 2253
40. G. ARZAMENDI and J. M. ASUA, *J. Appl. Polym. Sci*. **38** (1989) 2019
41. G. ARZAMENDI and J. M. ASUA, *Makromol. Chem., Macromol. Symp*. **35/36** (1990) 249
42. G. ARZAMENDI and J. M. ASUA, *Ind. Eng. Chem. Res*. **30** (1991) 1342
43. J. R. LEIZA, J. C. DE LA CAL, G. R. MEIRA and J. M. ASUA, *Polym. React. Eng*. **1**(4) (1993) 461
44. S. CANEGALLO, P. CANU, M. MORBIDELLI and G. STORTI, *J. Appl. Polym. Sci*. **54** (1994) 1919
45. M. VAN DEN BRINK, M. PEPERS, A. M. VAN HERK and A. L. GERMAN, *Polym. React. Eng*. **9**(2) (2001) 101
46. W. D. HERGETH, S. WARTEWIG, Z. RANACHOWSKI, J. RZESZOTARSKA and J. RANACHOWSKI, *Acta Polym*. **39** (1988) 677
47. K. HÖRNING, W. D. HERGETH and S. WARTEWIG, *Acta Polym*. **40** (1989) 257
48. A. URRETABIZKAIA, E. D. SUDOL, M. S. EL-AASSER and J. M. ASUA, *J. Polym. Sci. Pol. Chem*. **31** (1993) 2907
49. L. M. GUGLIOTTA, J. R. LEIZA, M. AROTÇARENA, P. D. ARMITAGE and J. M. ASUA, *Ind. Eng. Chem. Res*. **34** (1995) 3899
50. A. SALAZAR, V. D. G. GONZALEZ, L. M. GUGLIOTTA and G. R. MEIRA, in *Proceedings of the IV Simposio Argentino de Polúmeros*, Córdoba, Argentina, Nov. 1999, p. 157
51. V. D. G. GONZALEZ, L. M. GUGLIOTTA, J. R. VEGA and G. R. MEIRA, *J. Colloid Interf. Sci*. **285**(2) (2005) 581
52. A. SALAZAR, L. M. GUGLIOTTA, J. R. VEGA and G. R. MEIRA, *Ind. Eng. Chem. Res*. **37** (1998) 3582
53. L. M. GUGLIOTTA, G. ARZAMENDI and J. M. ASUA, *J. Appl. Polym. Sci*. **55** (1995) 1017
54. D. M. LANGE and G. W. POEHLEIN, *Polym. React. Eng*. **1**(1) (1992) 41
55. G. L. SHOAF, PhD dissertation (Georgia Institute of Technology, 1989)
56. M. L. LOPEZ DE ARABINA ECHEVERRÍA, Tesis Doctoral (Univ. del País Vasco, 1996)
57. J. L. GARDON, *J. Polym. Sci. Pol. Chem*. **6** (1968) 643
58. A. CRUZ RIVERA, L. RIOS-GUERRERO, C. MONNET, B. SCHLUN, J. GUILLOT and C. PICHOT, *Polymer* **60** (1989) 1873
59. F. R. MAYO and F. M. LEWIS, *J. Am. Chem. Soc*. **66** (1944) 1594
60. D. M. LANGE and G. W. POEHLEIN, *Polym. React. Eng*. **1**(1) (1992) 1
61. W. V. SMITH and R. H. EWART, *J. Chem. Phys*. **16** (1948) 592
62. J. UGELSTAD and F. K. HANSEN, *Rubber Chem. Technol*. **49** (1976) 536